Front. Phys. China (2006) 2: 230–237
DOI 10.1007/s11467-006-0016-x

RESEARCH ARTICLE

YANG Jing, CUI Lian-jun, XU Jian, CHENG Jian-chun

An inverse method of elastic constants for unidirectional fiber-reinforced composite plate

© Higher Education Press and Springer-Verlag 2006

Abstract An inverse method is presented to determine the elastic constants of an experimental sample, a titanium graphite unidirectional fiber-reinforced composite plate, using wavelet transform and neural networks. Optimal algorithms of wavelet transform and neural networks are given here in order to improve the accuracy of inversion results. Coherent results were shown in both fiber direction and cross fiber direction, proving the feasibility of this method. Neither the group velocity of the Lamb wave modes are needed, as in the conventional method，and no direct least-square fitting of the experimental waveforms is necessary.

Keywords composite material, inversion of elastic constants, wavelet transform, neural networks

PACS numbers 43.35.+d

1 Introduction

Composite material has been used widely in many industrial fields for years because of its unique advantages such as high stiffness, good fatigue resistance and so on. Laser ultrasonic [1–6] is also a powerful tool because it enables generation and detection of elastic waves in solids with minimum contact between the optical transducer and the surface thus providing a means to perform non-contact testing of materials and structures. This non-contact method is particularly well suited to analyze the elastic behavior [7–12] of new composite materials. Lamb wave is very useful in ultrasonic detection and many recent studies have been involved mainly with the quantitative determination of elastic constants and thickness of isotropic sheet materials [13–16] by the laser-generated Lamb wave. The measurement is based on the fact that, for a plate with the thickness much less than a wavelength, the transient waveform is characterized by the lowest Lamb wave modes. The first arrival is the lowest nondispersive symmetric mode (S_0) and it is followed by the dispersive lowest antisymmetric mode (A_0). This feature is utilized to measure thickness and elastic constants of isotropic materials without any prior knowledge of other acoustic parameters. However, the transient waveforms depend strongly on the longitudinal acoustic wavelength and the plate thickness. For plates with thickness on the order of millimeters, the transient waveforms excited by a laser pulse are much more complicated because of contributions from the higher-order Lamb wave modes. As each frequency component propagates with a different phase velocity, the initial shape of the transient waveform is temporally distorted and it is very difficult to extract enough useful information from such complicated signals using traditional signal processing methods such as Fourier transform.

The wavelet transform (WT) has been applied to analyze such signals with time-varying spectra in order to extract characteristics of transient Lamb waveforms [17–20]. Applications of artificial neural network (ANN) to quantitative nondestructive evaluation (QNDE) have been developed in recent years [21–25]. Ultrasonic Lamb wave methods are also studied extensively for characterizing elastic stiffness coefficients of composite materials in the fields of QNDE [26–28]. Research results indicate that it is often very difficult to invert directly the elastic properties of composite materials from dispersion curves or time-frequency representations. Thus, it is necessary to develop a method for extracting the elastic constants of composite plates directly from experimental laser-generated Lamb waveforms. This is the objective of this paper.

In this paper, a new inverse method of elastic constants

Translated from *Acta Acustica* ,2005, 30(4) (in Chinese)

Yang Jing (✉) , CUI Lian-jun, XU Jian, CHENG Jian-chun
Institute of Acoustics,Nanjing University,
Nanjing 210093, China
E-mail: yangj@nju.edu.cn

Received March 26, 2006

for a unidirectional fiber-reinforced composite plate directly from experimental transient Lamb waveforms generated and detected by lasers is presented, using a combination of neural networks and wavelet transforms. Four independent elastic constants have been inversed directly from experimental laser-generated Lamb waveforms in fiber direction [29]. On this basis, optimal algorithms of wavelet transform and neural networks are given here in order to improve the accuracy of inversion results. The sample library for learning and training networks is made up of theoretical transient Lamb waveforms obtained from theoretical simulations by employing the method of normal mode expansion [30,31] for analyzing laser generation process of the ultrasonic Lamb waves propagating along the principal directions in the fiber-reinforced composite plate, which can be modeled as a transversely isotropic medium. During the preprocessing of raw Lamb waveform signals, the basis wavelet function is changed and the method of discrete wavelet transform coefficients is employed to construct the eigenvector so as to extract useful information from raw signals and simplify the structure of neural networks. Influences of node numbers in the hidden layer on the performance of the whole network are analyzed and the network generalization is also discussed. Good results were shown in both fiber direction and cross fiber direction, proving the feasibility of this method.

2 Theoretical model

The unidirectional fiber-reinforced composite can be modeled as a transversely isotropic medium (six-angle-series crystal) bounded by two parallel surfaces with free of traction planes $x_3= \pm h$, $x_3=0$ being the mid-plane of the plate, as shown in Fig. 1. The coordinate axes x_1, x_2, and x_3 corresponding to the fiber, cross fiber and thickness directions, respectively, are the three principal directions. Supposed that the laser pulse is acted on the sample surface $(x_3=-h)$ in the thermoelastic field, a localized temperature variation in the sample induced by absorption of laser energy results in a localized thermal expansion, which, in turn, generates a transient displacement field $\boldsymbol{U}=(U_1, U_2, U_3)$. Lamb waves propagate along the x_1-direction, and then the total displacement field $\boldsymbol{U}=(U_1,U_2,U_3)$ is independent of x_2, so that the Lamb wave motion in the plane (x_1-x_3) is not coupled from the displacement component U_2 in the x_2

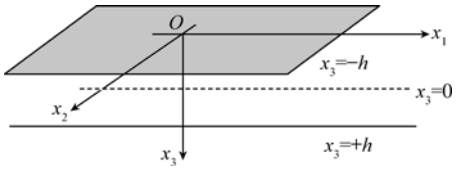

Fig.1 Orthotropic composite plate

direction. The transient displacement field in the plane (x_1-x_3) satisfies thermoelastic equation [30]

$$\rho\frac{\partial^2 U_1}{\partial t^2}=C_{11}U_{1,1}+C_{13}U_{3,1}+C_{55}(U_{1,3}+U_{3,1})+f_1 \quad (1)$$

$$\rho\frac{\partial^2 U_3}{\partial t^2}=C_{33}U_{3,3}+C_{13}U_{1,1}+C_{55}(U_{1,1}+U_{3,1})+f_3 \quad (2)$$

with the boundary conditions at $x_3=\pm h$,

$$C_{55}\left(U_{1,3}+U_{3,1}\right)=s_1,\quad C_{13}U_{1,1}+C_{33}U_{3,3}=s_3 \quad (3)$$

where ρ is the volume density of the plate, C_{ij} are elastic constants, $\boldsymbol{f}=(f_1, f_3)$ and $\boldsymbol{s}=(s_1,s_3)$ are the body and surface force density, respectively, induced by the laser pulse. Thus, the displacement field U_i can be expanded as

$$U_i(x_1,x_3,t)=\int_{-\infty}^{+\infty}\sum_n\frac{1}{m_n^2}\Phi_n(\omega_n,k,t)\psi_{in}(\omega_n,k,x_3)\times\exp(\mathrm{i}kx_1)\mathrm{d}k,\quad i=1,3 \quad (4)$$

where Φ_n and $\psi_n=(\psi_{1n}, \psi_{3n})^t$ are the generalized Fourier coefficients and Rayleigh-Lamb modes [30] respectively, and m_n is the norm of $\psi_n=(\psi_{1n}, \psi_{3n})^t$.

In order to increase efficiency of the ultrasonic excitation by a laser pulse, a very thin coating of oil at the generation spot has been used in the actual experimental system. Because thin coating of oil at the impinged generation spot is used to increase the acoustic generation efficiency from the laser pulse in experiments, both the evaporation and thermoelastic expansion effects of the oil will be considered in order to calculate the force sources at the same time. Evaporating force source can be dominated by a normal force monopole with $\delta(t)$ time dependence. This implies that the recoil force from ablation of the oil depresses the surface, and then rapidly returns to its equilibrium position. Therefore, the bulk force density $\boldsymbol{f}=0$ and the surface force density $\boldsymbol{s}=(0, s_3)$ is approximately proportional to the incident laser pulse

$$s_3(x_1,t)=\eta q_0 o(x_1)\delta(t) \quad (5)$$

where $o(x_1)$ is the spatial distribution of intensity of Gaussian pulse laser beam, η is the generation efficiency and q_0 is the totally absorbed laser energy.

For the thermoelastic expansion, a localized temperature variation θ in the sample induced by absorption of laser energy results in a localized thermal expansion, which, in turn, generates a transient displacement field U_i. The bulk and surface force densities resulting from the thermal stress are

$$f_i=\sum_{j=1,3}\beta_{ij}\frac{\partial\theta}{\partial x_j},\quad s_i=-\sum_{j=1,3}\beta_{ij}n_j\theta,\ i=1 \text{ and } 3 \quad (6)$$

where $(n_1,n_2,n_3)=(0, 0, \pm1)$ is the normal vector of the low and upper surfaces respectively, and β_{ij} is the stiffness thermoelastic expansion tensor.

The normal surface velocity (theoretical waveforms) can

be calculated numerically for certain elastic constants in both fiber direction and cross fiber direction, as shown in Fig. 2 and Fig. 3 respectively (*D* denotes the source-receiver distance). Compared to the latter Fig. 5 and Fig. 6, the theoretical results are in agreement with the experimental waveforms in the main characteristics, thus verifies the feasibility of the theoretical model proposed in this paper.

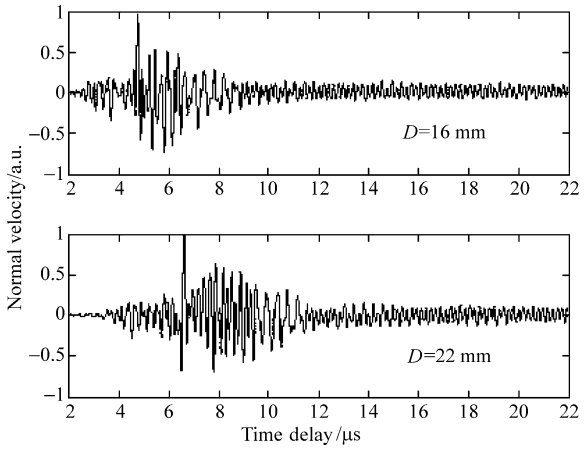

Fig.2 Theoretical Lamb waveforms propagating at the fiber direction (*D*=16 mm，22 mm)

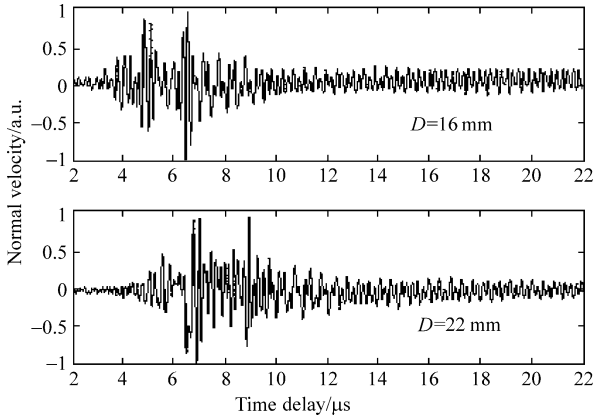

Fig.3 Theoretical Lamb waveforms propagating at the cross fiber direction (*D*=16 mm，22 mm)

3 Experimental system

The experimental configuration as shown in Fig. 4 is presented for the transient Lamb waves of pulse-laser generated and detected. The experimental sample is a titanium graphite unidirectional fiber-reinforced composite plate: SCS-6/Timetal 21S with a half thickness *h*=0.72 mm, which can be modeled as a transversely isotropic material if microstructure effects of ultrasonic waves is ignored. Thus there are only five independent elastic constants.

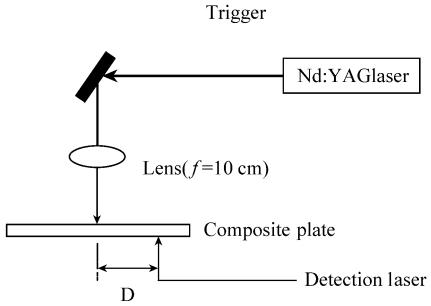

Fig. 4 Experimental configuration

The ultrasonic Lamb wave is generated by a Nd: YAG pulsed laser with an approximate duration of 10 ns and energy of 5.7 mJ (as shown in Fig. 4). The laser beam from the laser generator is first passing through the spectroscope, energy of which is mostly arriving the reflector through the spectroscope, partially is reflected upon the photo-electricity diodes by the spectroscope to trigger the oscillograph. The laser beam reflected by the reflector is focused on the experimental sample by a 10 cm focal-length lens. Size of the laser spot on the sample can be adjusted by the source-receiver distance, and the sample platform also can be translated and circumgyrated. The normal surface velocity of the ultrasonic Lamb waves at the rear surface is detected by a Michelson interferometer at different directions and locations (the source-receiver distance *D*) away from the pulsed laser spot, as shown in Fig. 5 and Fig. 6. In order to increase the efficiency of the ultrasonic excitation by a laser pulse, a very thin coating of silicon oil at the generation spot has been used in experiments.

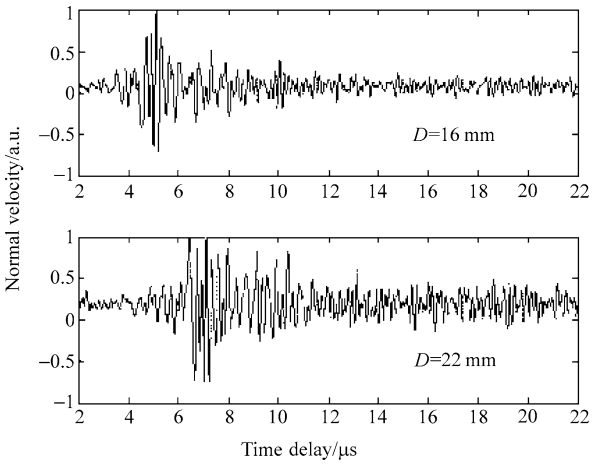

Fig.5 Experimental Lamb waveforms propagating at the fiber direction (*D*=16 mm，22 mm)

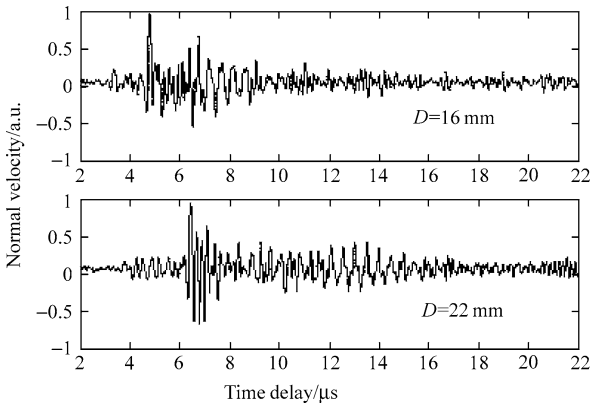

Fig.6 Experimental Lamb waveforms propagating at the cross fiber direction（*D*=16 mm，22 mm）

4 Improvement of inversion algorithms

In this paper, the overall inversion strategy for recovering the elastic constants of a composite plate is shown as Fig.7. The raw Lamb wave signals obtained by theoretical calculations are first preprocessed, which serves to extract the feature information of the transient waveforms so as to obtain the training sample for neural networks. The training sample, are then input to an appropriate network model designed for training and learning in order to ensure the network coefficients. At last, the experimental Lamb waveforms are used as input in the whole system to inverse elastic constants of the experimental material.

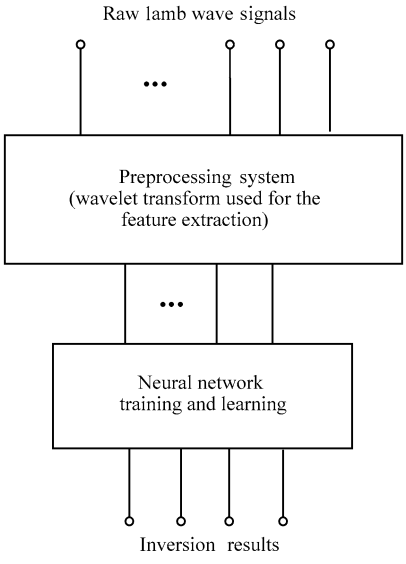

Fig.7 Overall inversion strategy to recover the elastic constants of a composite plate.

4.1 Data preprocessing

The wavelet transform[32] (WT), as well known, has been applied to analyze signals effectively in both time and frequency domains. However, for its scale is changed according to the binary system in wavelet analysis, it has relatively low frequency resolution at high frequency band and relatively low time resolution at low frequency band. The wavelet packet analysis method is a generalization of wavelet decomposition that offers a richer range of possibilities for signal analysis [33]. In wavelet packet analysis, the details as well as the approximations can be split, so it is a more complex and flexible analysis. The frequency band also can be chosen adaptively according to the spectrum feature of signals analyzed so as to increase both the time and frequency resolutions. Thus the wavelet packet analysis method is first adopted to construct the eigenvector [29] so as to extract the effective feature information of Lamb waves. But the further analysis indicates that, the discrete wavelet transform can extract the useful information of Lamb waves more effectively than the wavelet packet analysis method if wavelet basis function and corresponding scale coefficients are chosen properly. This method optimizes the data preprocessing to some extend and reduces the calculation load. In this paper, during the preprocessing of raw Lamb waveform signals, the basis wavelet function is changed and the method of discrete wavelet transform coefficients is employed to construct the eigenvector so as to extract useful information from Lamb waveform signals.

The discrete wavelet transform can be expressed as

$$\boldsymbol{w}[m,n]=a_0^{-m/2}\sum_k g^*\left[\frac{k-na_0^m b_0}{a_0^m}\right]f(k) \qquad (7)$$

where $f(k)$ is the raw signal to be processed, g is called as a basis or mother wavelet function which is chosen as Mexican Hat wavelet function in this paper in order to match the Lamb wave signals. a and b are the scale and translation coefficients respectively, m and n are discretization coefficients, $a=a_0^m$, $b=nb_0a_0^m$, $a_0>1$, $b_0>0$. Varieties of m change the filter characteristics and results of discrete wavelet transform for Lamb wave signals are shown as Fig.8. It can be seen, when m varies

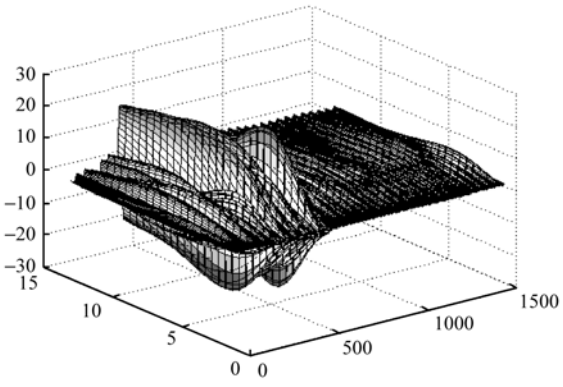

Fig.8 Results of discrete wavelet transform

from 1 to 13, energy of input signals is characterized obviously, especially at m=6. So in thereafter actual preprocessing, m is taken as a discrete value ranged from 1 to 13, and for each m value, corresponding coefficient $w(m,n)$ is calculated as n ranged from 1 to $length(f)$.

The procedure of extracting eigenvectors using WT consists of four steps as follows:

• Process the signals by discrete wavelet transform with a certain m value as m_0 =6;

• Transformed signals are divided into ten sections according to the time sequence, and total energy E_i of each section is computed;

• Construct the eigenvector as $\boldsymbol{T}=[E_1,E_2,E_3,E_4,E_5,E_6,E_7,E_8,E_9,E_{10}]$;

• Generalize the eigenvector according to $\boldsymbol{E}=\left(\sum_{i=1}^{10}|E_i|^2\right)^{\frac{1}{2}}$, and the generalized eigenvector is expressed as

$$\boldsymbol{T}=[E_1/E,E_2/E,E_3/E,E_4/E,E_5/E,E_6/E,E_7/E,E_8/E\cdots E_{10}/E]$$

4.2 Optimization of neural network architecture

The multi-layered feed-forward neural network architecture with back-propagation (BP) algorithm used here, as shown in Fig. 9, is composed of an input layer of nodes, a hidden layer and an output layer. The training algorithm used in this paper is Resilient Error Back-propagation algorithm [34]. Corresponding to the extraction method of above eigenvectors, input layer consists of 10 neurons. In order to prove the validity and generalization of neural network designed here, independent network architecture is adopted for fiber direction and cross fiber direction, respectively. The output layer consists of 4 neurons for fiber direction, each of which represents one of the four independent elastic constants C_{11}, C_{13}, C_{33}, C_{55}. In the same way, 4 output nodes are designed for cross fiber direction C_{22}, C_{23}, C_{33}, C_{44}. The validity of neural network designed in this paper can be judged from the agreement extent of C_{33} at two directions.

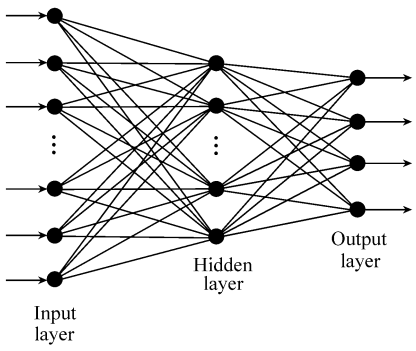

Fig.9 Architecture of multi-layer BP Network

BP network designed in this paper is composed of an input layer, a hidden layer and an output layer, where linear transfer functions are adopted in both input and output layers, nonlinear transfer function is adopted in the hidden layer. This structure is very effective for resolving problem such as a complicated function approach. Numbers of the neurons in input and output layers can be ensured by actual situation, but it is no certain theoretical criterion as to how to choose the number of neurons comprised in the hidden layer. In general, the number of neurons in the hidden layer is ascertained by experience. In the previous work, 12 hidden nodes were chosen by experience and the elastic constants were inversed from experimental waveforms at two detect distances (D=16 mm, 22 mm) in the fiber direction [29]. In this paper, further discussion as to how to choose the number of hidden nodes is studied. The number of hidden nodes is first set to 11, and then it is changed and network performances are compared under different situations so as to ascertain optimal number of hidden nodes. Error curves at the beginning of network training for different hidden nodes are shown as Fig.10, and corresponding curves at stabile stage of network training are shown as Fig.11.

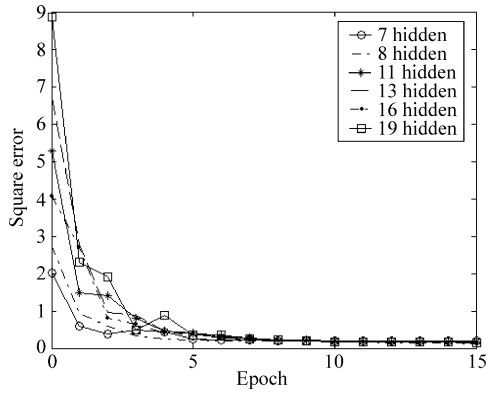

Fig.10 Error curves for different hidden nodes(at the beginning of network training)

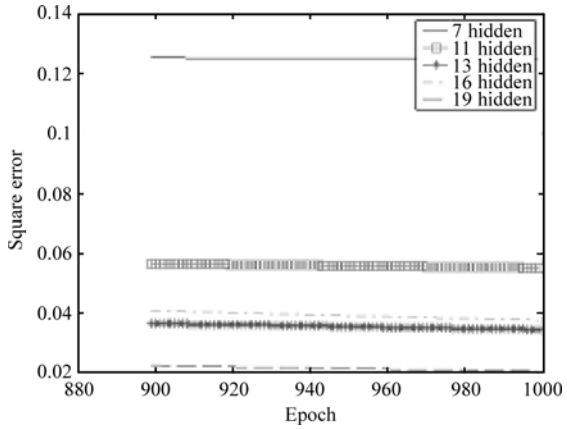

Fig.11 Error curves for different hidden nodes(at stabile stage of network training)

From Fig.11, it can be seen that the least mean square error is obtained as 19 hidden nodes are adopted. However, under this situation, quantity of samples used for training will be very large and the stability of neural network is relatively bad. So finally 13 hidden nodes are adopted in this paper. Figure10 also shows that, at the beginning of network training, the mean square error curve of network with 13 hidden nodes converges smoothly. In conclusion, the final BP network architecture is 10-13-4, which consists of 10 input nodes, 13 hidden nodes, and 4 output nodes.

5 Inversion results

5.1 Inversion of theoretical data

Transient Lamb wave signals can be obtained by numerical simulations for different elastic constants in both fiber and cross fiber directions. The total of 118 samples were obtained in fiber direction, where 100 samples were used for training and the remaining 18 samples were used for testing. The total of 116 samples were obtained in cross fiber direction, where 98 samples were used for training and the remaining 18 samples were used for testing. Some theoretical inversion results for fiber direction are shown in Table 1, where four elastic constants C_{11}, C_{13}, C_{33} and C_{55} are inversed; and some theoretical inversion results for cross fiber direction are shown in Table 2, where four elastic constants C_{22}, C_{23}, C_{33}, C_{44} are inversed.

Table 1 Inversion results of theoretical waveforms for fiber direction

	C_{11} /GPa	C_{13} /GPa	C_{33} /GPa	C_{55} /Gpa
Theoretical Value	241.0	86.9	152.0	44.6
Inversion Value	257.0	84.8	165.3	47.8
Inversion Error	6.2 %	2.5 %	8.1 %	6.7 %

Table 2 Inversion results of theoretical waveforms for cross fiber direction

	C_{22} /GPa	C_{33} /GPa	C_{23} /GPa	C_{44} /Gpa
Theoretical Value	259.0	180.0	90.0	47.0
Inversion Value	240.5	194.9	96.9	49.1
Inversion Error	7.7 %	7.6 %	7.1 %	4.3 %

Linear fit analysis curves of network output are shown as Fig.12. It can be seen that correlation coefficients between network outputs and target results are all above 0.9. This also proves generalization of network and feasibility of the inversion method proposed in this paper.

5.2 Inversion of experimental data

Finally, the experimental Lamb waveforms propagating along both fiber and cross fiber directions (D =16 mm) are used as inputs into the whole inversion system to determine the elastic constants of a fiber-reinforced composite plate. The inversion results of experimental waveforms for fiber and cross fiber direction are shown in Table 3 and Table 4, separately.

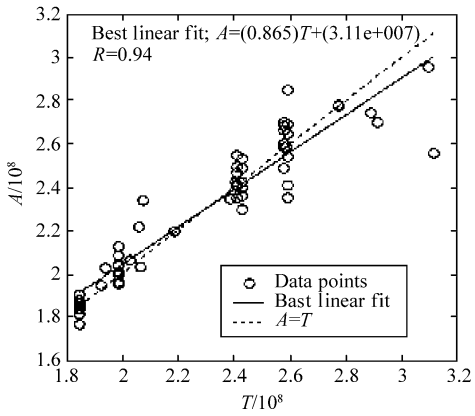

Fig.12 Linear fit analysis of inversion results for testing samples

Table 3 Inversion results of experimental waveforms for fiber direction

	C_{11} /GPa	C_{13} /GPa	C_{33} /GPa	C_{55} /Gpa
Inversion value	240.1	97.1	191.1	50.1

Table 4 Inversion results of experimental waveforms for cross fiber direction

	C_{22} /GPa	C_{33} /GPa	C_{23} /GPa	C_{44} /Gpa
Inversion value	206.1	198.6	100.6	42.4

Comparing the above inversion results, it can be seen that two sets of inverted constants C_{33} are in reasonable agreement with each other for their difference is within 4 %. This proves both the accuracy of network and the feasibility of this method used for inversing the elastic constants of composite plates by wavelet transform and artificial neural network. It also provides a basis for industrial applications of QNDE in composite plates.

6 Conclusions

In this paper, a new inverse method of elastic constants for a unidirectional fiber-reinforced composite plate using a combination of neural networks and wavelet transforms is presented. On the basis of previous study [29], optimization algorithms of wavelet transform and neural networks are presented here in order to improve the accuracy of inversion results. The elastic constants are inversed directly from experimental waveforms in the fiber and cross fiber direction, separately. Finally, inversion results in two directions are compared so as to prove the feasibility of the

network designed in this paper for engineering practice. The salient features of the method are as follows.

- The elastic constants of composite materials are directly recovered from the laser-generated transient Lamb waveforms by combining neural networks and wavelet transforms. Neither the phase or group velocity of the Lamb wave modes are needed, as in the conventional method, and no direct least-square fitting of the experimental waveforms is necessary. The latter is not only computationally too costly, but it also involves problems with the stability of the algorithm.
- The structure of the neural network is largely simplified by preprocessing with wavelet transforms to extract the eigenvectors from the Lamb wave signals, thus it can improve learning speed and accuracy of neural networks. The wavelet preprocessing technique shows great potential for analyzing transient Lamb wave signals with a wide frequency band. The major advantage of this technique is the ability to perform self-focus and multi-resolution analysis of the signal, and its structure of self-adaptive windows can resolve both the high and low frequency component of the signal which is just fit for analyzing the spectrum feature of transient Lamb wave signals.

Acknowledgements This work was supported by the National Natural Science Foundation of China (No. 10234060) and the Excellent Youth Science Foundation from the National Natural Science Foundation of China (No. 10125417).

References

1. J. Maynard, Resonant ultrasonic spectroscopy, Phys. Today, 1996, 49: 26–31
2. P. Heyliger et al, Elastic constants of isotropic cylinders using resonant ultrasound, J. Acoust. Soc. Am., 1993, 94: 1482–1487
3. A. Migliori and J.-L. Sarao, Resonant ultrasound spectroscopy, New York: Wiley, 1997
4. C. Remken et al, An experimental evaluation of the resonant ultrasonic spectroscopy method, in: Review of Progress in Quantitative NDE, edited by D. O. Thomposon and D. E. Chimenti(Plenum, New York, 1998), 17B: 2029–2044
5. C.-B. Scruby, R.-J. Dewhurst, and S.-B. Palmer, Quantitative studies of thermally generated elastic waves in laser-irradiated metals, J. Appl. Phys., 1980, 51: 6210–6216
6. C.-B. Scruby and L.-E. Drain, Laser Ultrasonics Techniques and Applications, Hilger, Bristol, 1990
7. S. Guilbaud and B. Audoin, Measurement of the stiffness coefficients of a viscoelastic composite material with laser-generated and detected ultrasound, J. Acoust. Soc. Am., 1999, 105: 2226–2235
8. B. Audoin and C. Bescond, Measurement by laser-generated ultrasound of four stiffness coefficients of an anisotropic material at elevated temperatures, J. Nondestruct. Eval., 1997, 16: 91–100
9. B. Audoin, C. Bescond, and M. Deschamps, Measurement of stiffness coefficients of anisotropic materials from point-like generation and detection of acoustic waves, J. Appl. Phys., 1996, 80: 3760–3771
10. Y.-C. Chu and S.-I. Rokhlin, A Method for determination of elastic constants of a unidirectional lamina from ultrasonic bulk velocity measurements on [0/90] cross-ply composites, J. Acoust. Soc. Am., 1994, 96: 342–352
11. A.-G. Every and W. Sachse, Determination of the elastic constants of an anisotropic solid from acoustic-wave group-velocity measurements, Phys. Rev., 1990, B42: 8196–8205
12. T.-T. Wu and Y.-H. Liu, On the measurement of anisotropic elastic constants of fiber-reinforced composite plate using ultrasonic bulk wave and laser generated Lamb wave, Ultrasonics., 1999, 37: 405–412
13. H. Sontag and A.-C. Tam, Optical monitoring of photoacoustic pulse propagation in silicon wafers, Appl. Phys. Lett., 1985, 46: 725–727
14. R.-J.Dewhurst, C.Edwards, A.-D.-W.Mckie and S.-B. Palmer, Estimation of the thickness of thin metal sheet using laser generated ultrasound, Appl. Phys. Lett., 1987, 51: 1066-1068
15. D.-A. Hutchins, K. Lundgren and S.-B. Palmer, A laser study of transient Lamb waves in thin materials, J. Acoust. Soc. Am., 1989, 85: 1441–1448
16. L.Noui and R.-J.Dewhurst, Two quantitative optical detection techniques for photoacoustic Lamb waves, Appl. Phys. Lett., 1990, 57: 551–553
17. J.Chao, L.Udpa and S.-S. Udpa, Ultrasonic signal analysis using wavelet transform, Rev. Prog. Quant. Nondestru. Eval., 1996, 12: 735–742
18. T. Onsay and A.-G. Haddow, Wavelet transform analysis of transient wave propagation in a dispersive medium, J. Acoust. Soc. Am., 1994, 95: 1441–1448
19. A.Abbate, J.Frankel and P.Das, Wavelet transform signal processing applied to ultrasonics, Rev. Prog. Quant. Nondestru. Eval., 1996, 15, 741–748
20. J.-B.Han, J.-C.Cheng, T.-H.Wang and Y.Berthelot, Mode analyses of laser-generated transient ultrasonic Lamb waveforms in a composite plate by wavelet transform, Mater. Eval., 1999, 57, 837–840
21. J.-J. Thomsen and K. Lund, Quality control of composite materials by neural network analysis of ultrasonic power spectra, Mater. Eval., 1991, 49: 594–600
22. L.Udpa and S.-S.Udpa, Neural networks for the classification of nondestructive evaluation signals, IEEE Proc. –F, 1991, 138: 41–45
23. C.-G.Windsor, F.Anselme, L.Capineri, and J.-P.Mason, The classification of weld defects from ultrasonic images: A neural network approach, Br. J. NDT., 1993, 35: 15–22
24. R.-E.Challis, U. Bork and C.-P. -D. Todd, Ultrasonic NDE of adhered T-joints using Lamb waves and intelligent signal processing, Ultrasonics., 1996, 34: 455–459
25. C.-P. -D. Todd and R.-E. Challis, Quantitative classification of adhesive bondline dimensions using Lamb waves and artificial neural networks.,IEEE Trans.UFFC., 1999, 46: 167–181
26. LIU Zhenqing, HUANG Ruiju, Experimental analysis of acousto-ultrasonic wave propagation mode in thin plate, Acta Acustica(in Chinese), 2000; 25(3): 268–273
27. ZHANG RUI，WAN Mingxi，LI Gang，CAO Wenwu, Low frequency ultrasonic multi-mode Lamb wave method for characterizing the ultra-thin transversely isotropic laminate composite: theory and experiment, Acta Acustica(in Chinese), 2001, 26(1): 79–84
28. LIU Zhenqing，LIU Xiao, TA De'an, Inverse determinations of the parameters of three-layered plate using angle probe generated Lamb waves, Acta Acustica(in Chinese), 2002, 27(5): 408–412
29. Jing Yang, Jianchun Cheng and Yves Berthelot, Determination of the elastic constants of a composite plate using wavelet transforms and neural networks, J. Acoust. Soc. Am., 2002, 111: 1245–1250
30. J.-C. Cheng and Y. Berthelot, Theory of laser-generated transient Lamb waves in orthotropic plates, J. Phys. D: Appl. Phys., 1996, 29: 1857–1864

31. J.-C. Cheng, S.-Y. Zhang and Y. Berthelot, Experimental and theoretical analyses on laser-generated Lamb waves in an orthotropic plate, Rev. Prog. Quant. Nondestru. Eval., 2000, 19: 1151–1158
32. Ingrid Daubechies, The wavelet transform, time-frequency localization and signal analysis, IEEE Trans. Inform. Theory., 1990, 36: 961–1003
33. B.Carnero and A. Drygajlo, Fast short-time orthogonal wavelet packet transform algorithms, Proc. ICASSP, 1995, 1161–1164
34. R.-J. Schalkoff, Artificial Neural Networks, New York: McGraw-Hill, 1997